Polymerization of Supramolecular Diacetylenic Monomer Embedded in Porous Silicon Matrix

Luc Vellutini,*,† Nicolas Errien,† Gérard Froyer,† Nelly Lacoudre,‡ Sylvie Boileau,‡ François Tran-Van,§ and Claude Chevrot§

Laboratoire de Physique des Matériaux et Nanostructures, Institut des Matériaux Jean Rouxel, UMR 6502, 44322 Nantes, France, Laboratoire de Recherche sur les Polymères, UMR C 7581, 94320 Thiais, France, and Laboratoire de Physico-chimie des Polymères et des Interfaces, EA 2528, 95031 Cergy-Pontoise, France

We have used a porous silicon matrix filled with polydiacetylenic derivatives to obtain new nanocomposites. The polymerization, known as a topochemical process, requires optimal packing of the diacetylenic segments to allow polymerization propagation across the assembly to give a conjugated backbone. We have explored the use of intermolecular H-bond interactions between diacetylenic diacid monomers to control the polymer chain organization after the polymerization step. Resonance Raman and IRTF spectroscopy have been used to directly probe the diacetylenic segment of the monomer and the pendent side-chain arrangement. Diacetylenic derivatives have been successfully incorporated inside the pores after a specific chemical treatment to improve the filling rate of the monomer. Polarized Raman scattering indicated that the monomers have a preferential orientation along the pore axis, probably because of the confinement effect and hydrogen bonding of the self-associated carboxylic dimeric form. After the polymerization process, resonance Raman spectroscopy shows a highly oriented ene−yne backbone characterized by a blue phase.

Introduction

Over the past few years, there has been an increasing interest in polymeric materials, which present applications in the field of NLO, electronic, and electro-optical devices.[1−6] Polydiacetylenes are the most widely investigated class of conjugated polymers for third-order nonlinear optical effect. The development of future application supposes a control of the properties of the material and thus the ordering of the molecular structure. It is well-known that diacetylenic monomers can undergo photopolymerization to form an ene−yne alternated polymer chain upon UV irradiation in a wide range of organized structures, such as single crystals,[7] crystallite in nanoporous substrate,[8] Langmuir−Blodgett films,[9] self-assembled monolayers,[10] liposomes or vesicles[11] and solutions.[12] The one-dimensional conjugated polyenyne backbone exhibits large nonlinear optical susceptibilities comparable to inorganic semiconductors with ultrafast response time.[13,14] Many derivative polymers have drawn considerable attention to understanding the mechanism of the polymerization reaction, which has been found to depend on the orientation and packing of diacetylenic derivatives.[15−20]

* Corresponding author. E-Mail: l.vellutini@lcoo.u-bordeaux1.fr. Tel: 33240373988. Fax: 33240373991.
† Laboratoire de Physique des Matériaux et Nanostructures.
‡ Laboratoire de Recherche sur les Polymères.
§ Laboratoire de Physico-chimie des Polymères et des Interfaces.

(1) Patil, A. O.; Heeger, A. J.; Wuld, F. *Chem. Rev.* **1988**, *88*, 183.
(2) Nalwa, H. S. *Adv. Mater.* **1993**, *5*, 341.
(3) Sauert, C.; Herman, J. P.; Fer, R.; Predieere, F.; Ducing, J.; Baughman, R. H.; Chance, R. R. *Phys. Rev. Lett.* **1976**, *36*, 956.
(4) Bloor, D.; Chance, R. R., Eds. *Polydiacetylenes*; Martinus Nijhoff: Dordrecht, The Netherlands, 1985.
(5) Chemla, D. S.; Zyss, J., Eds. *Nonlinear Optical Properties of Organic Molecules and Crystals*; Academic Press: Orlando, FL, 1987.
(6) Kasai, H.; Tanaka, H.; Okada, S.; Oikawa, H.; Kawai, T.; Nakanishi, H. *Chem. Lett.* **2002**, *31*, 696.
(7) (a) Donovan, K. J.; Wilson, E. G. *Synth. Met.* **1989**, *28*, D563−D568. (b) Koshihara, S.; Tokura, Y.; Takeda, K.; Koda, T.; Kobayashi, A. *J. Chem. Phys.* **1990**, *92*, 7581−7588. (c) Tashiro, K.; Nishimura, H.; Kobayashi, M. *Macromolecules* **1996**, *29*, 8188−8196.
(8) Wang, Y.; Yang, K.; Kim, S.-C.; Nagarajan, R.; Samuelson, L. A.; Kumar, J. *Chem. Mater.* **2006**, *18*, 4215.
(9) (a) Tieke, B.; Graf, H. J.; Wegner, G.; Naegele, B.; Ringsdorf, H.; Banerjie, A.; Day, D.; Lando, J. B. *Colloid Polym. Sci.* **1977**, *255*, 521−531. (b) Berman, A.; Ahn, D. J.; Lio, A.; Salmeron, M.; Reichert, A.; Charych, D. *Science* **1995**, *269*, 515−518. (c) Kuriyama, K.; KiKuchi, H.; Kajiyama, T. *Langmuir* **1998**, *14*, 1130−1138.
(10) (a) Batchelder, D. N.; Evans, S. D.; Freeman, T. L.; Häussling, L.; Ringsdorf, H.; Wolf, H. *J. Am. Chem. Soc.* **1994**, *116*, 1050−1053. (b) Mowery, M. D.; Menzel, H.; Cai, M.; Evans, C. E. *Langmuir* **1998**, *14*, 5594−5602.
(11) (a) Singh, A.; Thompson, R. B.; Schnur, J. M. *J. Am. Chem. Soc.* **1986**, *108*, 2785−2787. (b) Okada, S.; Peng, S.; Spevak, W.; Charych, D. *Acc. Chem. Res.* **1998**, *31*, 229−239.
(12) Donovan, K. J.; Wilson, E. G. *Synth. Met.* **1989**, *28*, D569−D574.
(13) Prasad, P. N.; Williams, D. L. *Introduction to Nonlinear Optical Effect in Molecules & Polymers*; John Wiley & Sons: New York, 1991; pp 231−235.
(14) (a) Agrawal, G. P.; Cojan, C.; Flytzanis, C. *Phys. Rev. B* **1978**, *17*, 776−789. (b) Huggins, K. E.; Son, S.; Stupp, S. I. *Macromolecules* **1997**, *30*, 5305−5312.
(15) Tieke, B.; Wegner, G.; Naegele, D.; Ringsdorf, H. *Angew. Chem., Int. Ed.* **1976**, *15*, 764.
(16) Batchelder, D. N.; Evans, S. D.; Freemen, T. L.; Häussling, L.; Ringsdorf, H.; Worf, H. *J. Am. Chem. Soc.* **1994**, *116*, 1050.
(17) Kanetake, T.; Tokura, Y.; Koda, T. *Solid State Commun.* **1985**, *56*, 803.
(18) Kim, T.; Crooks, R. M.; Tsen, M.; Sun, L. *J. Am. Chem. Soc.* **1995**, *117*, 3963.
(19) Mowery, M. D.; Kopta, S.; Ogletree, D. F.; Salmeron, M.; Evans, C. E. *Langmuir* **1999**, *15*, 5118.
(20) Britt, D. W.; Hofmann, U. G.; Möbius, D.; Hell, S. W. *Langmuir* **2001**, *17*, 3757.

We were interested in preparing oriented polydiacetylene for optical and electronic applications. To control the polymerization direction, we proposed to use an anisotropic substrate, mesoporous silicon. The structure of porous silicon is well-known from transmission electron microscopy to consist of narrow (nanometer-scale) pores running normal to the silicon surface.[21] Porous silicon (PSi) has been widely investigated for a number of electronics and optoelectronics applications.[22–24] The porous layer is a large-surface-area matrix that is prepared by chemical and/or electrochemical etching of single-crystal Si wafer in HF-based solutions. One of the benefits in using porous silicon as a substrate is the ability to control the size of the pores and thickness of the porous layer by choosing the appropriate etching parameters.

We have demonstrated that it is possible to obtain novel nanocomposite materials by embedding uniformly conjugated polymers into porous silicon using either an electrochemical or chemical method.[25,26] Both methods allow obtaining an homogeneous layer of hybrid material with a large third-order nonlinear coefficient.[27] We have also determined the orientation of macromolecular chains of PDA-TS along the pore axis pointing out a confinement effect.[28] These results are particularly encouraging but indicate clearly that the macromolecular organization has to be improved within the pores of the matrix.

Here, we report for the first time the introduction of the self-assembled diacetylenic monomer 10,12-docosadiynedioic acid (HOOC$-$(CH$_2$)$_8$$-C\equiv$C$-C\equiv$C$-$(CH$_2$)$_8$$-$COOH) by hydrogen bonds in the porous silicon layer, in order to reach a better macromolecular organization after the polymerization step. In this study, FTIR absorption spectroscopy was used to probe the influence of the surface chemistry on the pore filling. Raman scattering spectroscopy was also used to determine the structural organization of the self-assembled diacetylenic monomer.

Experimental Section

General Information. Chloroform (Aldrich), sulfuric acid (95–97%, Fluka), hydrogen peroxide (35%, Labogros) were used as received. 10,12-Docosadiynedioic acid was available from Lancaster and used as received. Single-side polished silicon wafer was purchased from Siltronix.

Porous Silicon Etching Procedure.[29,30] Highly bore-doped p-type silicon (<100>, $\rho = 3-7$ mΩ/cm) was used to prepare porous silicon samples by anodic etching in a fluorhydric acid solution (2:2:1 48% HF:deionized water:ethanol, v/v/v). *Caution: the HF solutions are hazardous and were always handled in an efficient fume hood.* Wafers (100 mm) were cut into 1.5 cm × 1.5 cm pieces. Porous silicon layers were fabricated at constant current density of 100 mA cm^{-2} for 240 s, giving a porosity of 80% under these experimental conditions. The pore diameter ranges from 20 to 50 nm, and the porous layer is 10 μm thick. The etched wafer was removed from the cell, rinsed with deionized water several times, and dried under vacuum. Prior to use, the samples are treated for a few seconds in a SF$_6$ plasma to make sure that the pores are opened properly on the silicon surface.

Sample Preparation. Prior to pore filling, most of the substrates were oxidized with a freshly prepared (7:3 H$_2$SO$_4$:H$_2$O$_2$ v/v) Piranha solution (*caution: this mixture reacts violently with organic materials and must be handled with great care*) for 15 min at room temperature, followed by being rinsed extensively with deionized water and dried under vacuum. This pretreatment makes the porous silicon surface rich in hydroxyl groups, as verified by ATR-FTIR (see below).

After this pretreatment, the porous silicon samples were first covered with a thin film of monomer powder and then pumped under vacuum to eliminate molecules adsorbed in the porous matrix. The monomer powder was heated above its melting point (116 °C), and the as-obtained liquid can thus fill up the pores. At this temperature, the polymerization does not occur, as checked by Raman Scattering spectroscopy. After being cooled to room temperature, the sample was exposed to UV light (254 nm, MHL 470 type 400 W medium-pressure mercury lamp) in air to initiate the polymerization.

Surface Characterization. IR data were obtained by attenuated total reflection (ATR) configuration using a set up equipped with a diamond crystal on a Nicolet FTIR spectrophotometer with a MCT detector at 4 cm^{-1} resolution. Raman spectra obtained with the excitation line in the visible range ($\lambda_{exc} = 676.4$ nm) were recorded on a multichannel Jobin-Yvon T64000 type spectrometer (4 cm^{-1} resolution). Scanning electron microscopy (SEM) images were obtained with a JEOL 6500 field emission microscope, using an accelerating voltage of 7.0 keV. Transmission electronic microscopy (TEM) images were obtained with a JEOL 200 CX microscope.

Results and Discussion

Filling of Porous Silicon. The introduction of the monomer into the pores of porous silicon depends on the surface properties and chemistry. Freshly etched SiHx-terminated porous silicon (Sip$-$H) is hydrophobic. According to the mechanism of porous silicon formation, the pore walls are depleted in majority carriers, leading to a porous silicon layer sufficiently transparent in the IR region to allow spectra acquisition by ATR mode FTIR spectroscopy.[31] The FTIR spectrum in ATR mode of a freshly etched porous silicon layer (Figure 1a) shows the ν Si$-$Hx stretching modes at 2090 cm^{-1}. Additional absorptions are present at 906 and 620 cm^{-1}, corresponding to the δ SiH$_2$ and δ SiH scissor mode, respectively. Attempts to fill the 10,12-docosadiynedioic acid inside the Sip$-$H pores probably failed because of the weak affinity of the hydrophilic monomer for the hydrophobic substrate. Consequently, it is necessary to modify the chemical nature of the pore surface to optimize the filling of the monomer into the porous structure. The

(21) (a) Sailor, M. J.; Lee, E. J. *Adv. Mater.* **1997**, *9*, 783. (b) Sailor, M. J.; Heinrich, J. L.; Lauerhaas, J. M. *Stud. Surf. Sci. Catal.* **1997**, *103*, 209. (c) Buriak, J. M. *Chem. Commun.* **1999**, 1051.
(22) Canham, L. T. *Appl. Phys. Lett.* **1990**, *57*, 1046.
(23) Canham, L. T. Ed. *Properties of Porous Silicon;* INSPEC: London, 1997; Vol. 18.
(24) Cullis, A. G.; Canham, L. T.; Calcott, P. D. *J. Appl. Phys.* **1997**, *82*, 909.
(25) Errien, N.; Vellutini, L.; Froyer, G.; Louarn, G.; Simos, C.; Skarka, V.; Haesaert, S.; Joubert, P. *Phys. Status Solidi C* **2005**, *2* (9), 3218.
(26) Errien, N.; Joubert, P.; Chaillou, A.; Mahric, C.; Godon, C.; Louarn, G.; Froyer, G. *Mater. Sci. Eng., B* **2003**, *100*, 259.
(27) Simos, C.; Rodriguez, L.; Skarka, V.; Nguyen Phu, X.; Errien, N.; Froyer, G.; Nguyen, T. P.; Le Rendu, P.; Pirastesh, P. *Phys. Status Solidi C* **2005**, *2* (9), 3232.
(28) Errien, N.; Mevellec, J.-Y.; Froyer, G.; Louarn, G. *Chem. Mater.* **2005**, *17* (11) 2803.
(29) Schultze, J. W.; Jung, K. G. *Electrochim. Acta* **1995**, *40*, 1369.
(30) Errien, N.; Mevellec, J.-Y.; Louarn, G.; Froyer, G. *Chem. Mater.* **2005**, *17*, 2803.

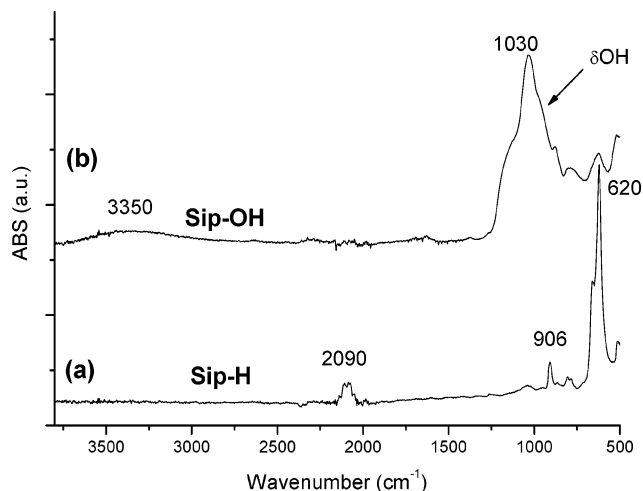(31) Bisi, O.; Ossicini, S.; Pavesi, L. *Surf. Sci. Rep.* **2000**, *38*, 1.

Figure 1. ATR infrared absorption spectra of a porous silicon sample. (a) Silicon layer freshly etched at 100mA/cm^2 for 4 min, (b) after oxidation with a Piranha solution.

hydrogen-terminated porous silicon (Sip−H) was oxidized with a Piranha solution to generate the silanol groups. Figure 1b displays a ATR mode FTIR spectrum of a modified porous silicon surface (Sip−OH) after treatment. The spectrum shows a significant oxidation of the surface, as seen from the large increase in the Si−O stretching mode near 1030 cm^{-1}. The stretching vibration band of the OH is also present close to 3350 cm^{-1}. The shoulder between 850 and 980 cm^{-1} can be assigned to δ OH (SiOH). The porous silicon surface covered by the silanol groups can interact by intermolecularly hydrogen bonding with the carboxylic groups of the monomer.

The results of porous silicon filling by the diacetylenic diacid monomer can be checked on a cleaved layer by using Raman scattering measurements.

Figure 2a clearly shows the presence of diacetylenic diacid monomer in the pores. The characteristic bands at δ_{COH} (1443 cm^{-1})[32] and $\nu_{C\equiv C}$ (2091 cm^{-1}) can be observed at the same position in the nanocomposite and in the pure monomer (not shown here). The peak at 521 cm^{-1} corresponds to the stretching vibration of the Si−Si bond.[33] To estimate the quantitative filling of the pores with the monomer, we used the surface peak ratio δ_{COH}/ν_{Si} from Raman spectra, which corresponds to the filling factor. Figure 2b shows that the filling is not homogeneous in the porous layer. We can observe a decrease in the amount of monomer from the top to the bottom of the pores.

The transmission electron microscopy (TEM) image (Figure 3a) shows the rough surface of the pores. The diameter of the pores can vary between 20 and 50 nm (Figure 3b). However, it can be seen that a diameter of 20 nm constitutes bottlenecks that prevent a complete filling of the pore bottom. This rough texture of the pores can thus explain the non-homogeneous filling through the whole depth of the pores.

Structural Organization of the Monomer. At this point, it is interesting to check whether the monomer presents a

(32) Megherbi, A.; Grande, D.; Lacoudre, N.; Boileau, S. World Polymer Congress, MACRO IUPAC, July 4−9, 2004, Paris.
(33) Kang, Y.; Qiu, Y.; Lei, Z.; Hu, M. *Opt. Lasers Eng.* **2005**, *43* (8), 847.
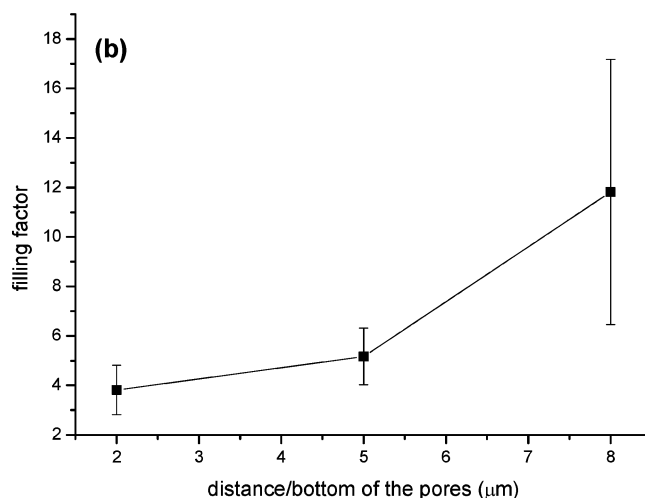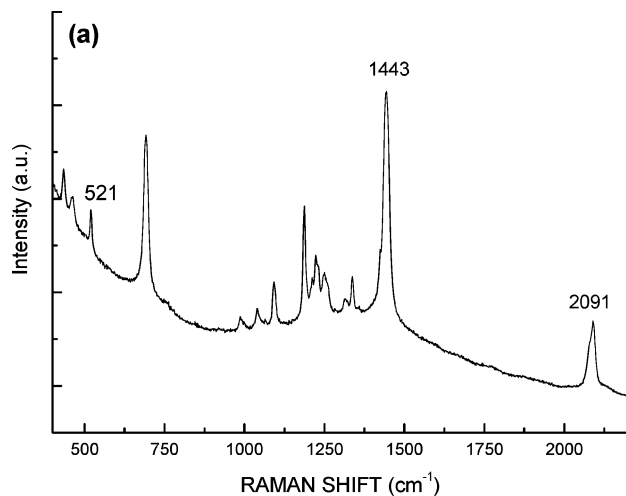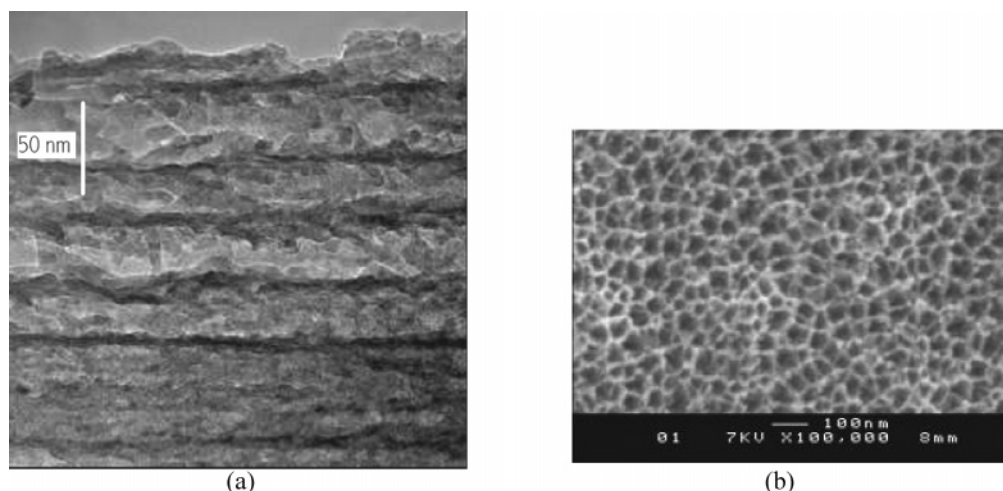

Figure 2. (a) Resonance Raman spectra of monomer inside the pores. (b) Concentration profile of the monomer inside the porous silicon layer obtained by Raman scattering spectroscopy on a cleaved layer. The filling factor corresponds to the peak area δ_{COH}/ν_{Si} ratio.

particular organization in the pores. This study was achieved by polarized micro-Raman scattering on the cleaved layer. Polarized incident light direction was fixed by using the parallel/parallel (source and analyzer) orientation and the sample was rotated around the same point with an amplitude of 90°. Figure 4 shows the integrated intensity evolution of the $\nu_{C\equiv C}$ (2091 cm^{-1}) Raman band as a function of the polarization angle. The intensity is minimum for a polarization which is perpendicular to the pore axis. On the other hand, the intensity is maximum for a polarization parallel to the pore axis. Consequently, there is on average a preferential orientation of the monomer along the pore axis, because the observed mode is polarized along the molecule long axis.

The existence of self-assemblies of the monomer in the silicon layer was evidenced by FTIR measurements in the ATR mode (Figure 5a). Carboxylic acids are well-known to exist under the hydrogen-bonded dimeric form. The C=O and O−H stretching vibration bands of the terminal carbonyl and carboxyl groups directly reflect the formation of hydrogen bonds. A peak at 1690 cm^{-1} for the carbonyl stretching and the broad band centered at 3000 cm^{-1} for the

Figure 3. (a) TEM image of side view and (b) SEM image of the surface of porous silicon layer after treatment to open the pores.
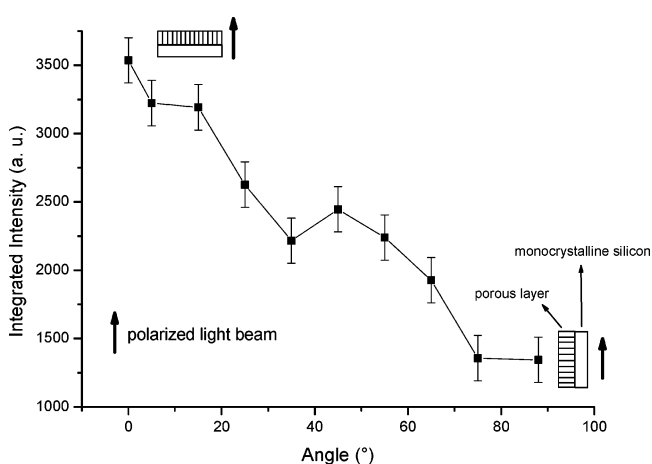

Figure 4. Intensity evolution of the 2091 cm^{-1} band as a function of monomer orientation inside a porous silicon layer measured by polarized Raman scattering spectroscopy ($\lambda = 676.4$ nm).
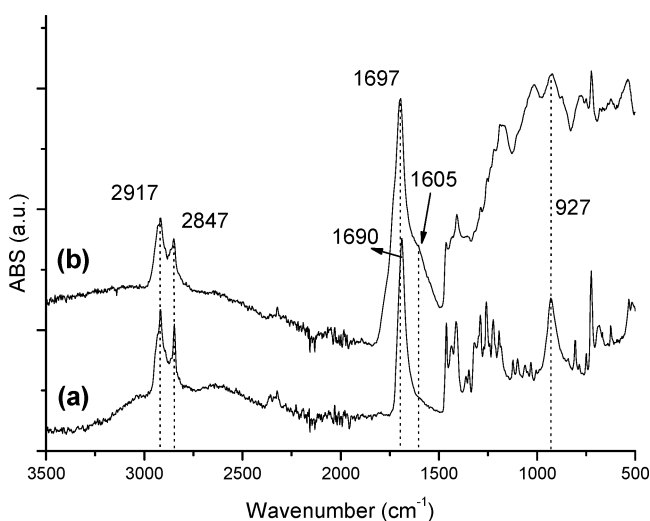

Figure 5. ATR infrared absorption spectra of a nanocomposite sample. (a) Diacetylenic monomer in a porous layer, (b) polymer in a porous layer after UV irradiation (polymerization).

O−H stretching were indicative of the hydrogen-bonded dimer of the carboxylic acid molecules.[34] Further support for the dimer structure is given by the appearance of a strong

peak at 927 cm^{-1}, characteristic of the out-of-plane O−H bending mode in the acid dimer.[35]

Specific information about the conformation state of the alkylene chain can be obtained from the middle infrared measurements. The frequency, width, and intensity of the asymmetric (ν_{as} CH$_2$) and symmetric (ν_s CH$_2$) methylene stretching bands near 2920 and 2850 cm^{-1} are sensitive to the gauche/trans conformer ratio and to the packing density of alkylene chains, respectively.[36] Shifts to lower frequencies for the ν_{as}(CH$_2$) vibration are indicative of highly ordered conformations with preferential all-trans configuration.[37] In contrast, the frequency and width of ν_{as}(CH$_2$) increase with the chain disorder. For example, the crystalline *n*-alkanes exhibit a band at 2920 cm^{-1}, whereas this band upshifts to 2928 cm^{-1} for liquid *n*-alkanes.[38] From Figure 5a, the monomer shows strong absorption bands at 2917 and 2847 cm^{-1}, which can be attributed to asymmetric ν_{as}(CH$_2$) and symmetric ν_s(CH$_2$) stretching vibrations, respectively. These frequencies are characteristic of highly ordered all-trans conformations of methylene chains.[37] The alkylene segments (CH$_2$)$_8$ exhibit good Van der Waals interactions between the alkyl chains and permit an efficient chain packing.

Photopolymerization. Chain polymerization can be induced by ultraviolet irradiation of the monomer introduced inside the pores. The porous layer was irradiated with ultraviolet light (254 nm). Polydiacetylenes are known to exist in several chromatic phases that appear as blue or red.[39−41] The exact nature of this chromism is generally attributed to variations in the polymer conjugation lengths. The backbone of the blue phase is highly oriented and shows

(34) Colthup, N. B.; Daly, L. H.; Wiberley, S. E. *Infrared and Raman Spectroscopy,* 3rd ed.; Academic Press: New York, 1990.

(35) Hadzi, D.; Sheppard, N. *Proc. R. Soc. London, Ser. A* **1953**, *216*, 247.
(36) Vaia, R. A.; Teukolsky, R. K.; Giannelis, E. P. *Chem. Mater.* **1994**, *6*, 1017.
(37) MacPhail, R. A.; Strauss, H. L.; Snyder, R. G.; Elliger, C. A. *J. Phys. Chem.* **1984**, *88*, 334.
(38) Snyder, R. G.; Strauss, H. L.; Elliger, C. A. *J. Phys. Chem.* **1962**, *86*, 5145.
(39) Menzel, H.; Mowery, M. D.; Cai, M.; Evans, C. E. *J. Phys. Chem. B* **1998**, *102*, 9550.
(40) Menzel, H.; Horstmann, S.; Mowery, M. D.; Cai, M.; Evans, C. E. *Polymer* **2000**, *41*, 8113.
(41) Semaltianos, N. G.; Araujo, H.; Wilson, E. G. *Surf. Sci.* **2000**, *460*, 182.

Polymerization of Supramolecular Diacetylenic Monomer

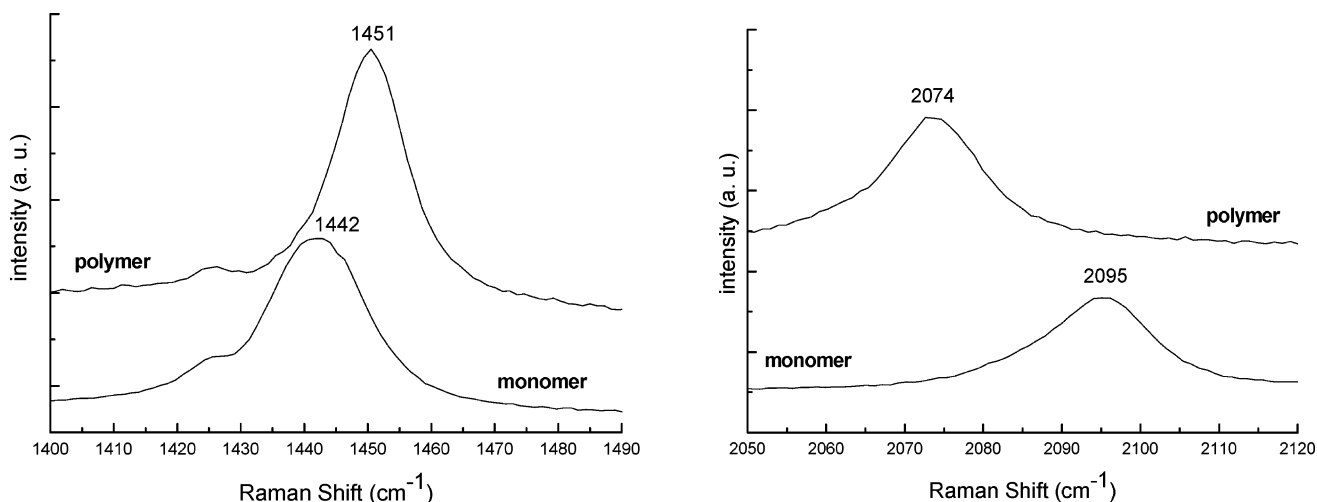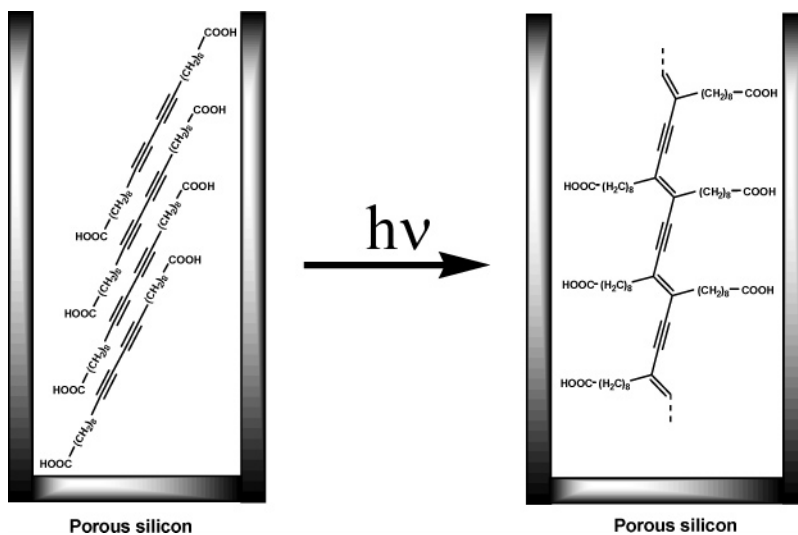*Chem. Mater., Vol. 19, No. 3, 2007* 501

Figure 6. Resonance Raman spectra of the polymer as compared to that of the monomer within the porous silicon ($\lambda = 676.4$ nm).

Scheme 1. Topochemical Photopolymerization of Polydiacetylene Derivatives in the Porous Layer

high conjugation lengths.[42−44] In contrast, the red phase is characterized by a partly disordered backbone, with relatively short conjugation lengths. To establish the presence of polymer inside the pores, we have used resonance Raman spectroscopy on a cleaved layer nanocomposite. This technique directly probes the polymerized ene−yne chromophoric units but not the pendent side-chain conformation. For the polymer, Figure 6 shows peaks at 1451 and 2074 cm^{-1} corresponding to the C=C and C≡C stretching modes, respectively, of the blue-phase polymer.[45] Analyses along the pore axis have revealed only one blue phase, indicating a high conjugation length and an homogeneous polymerization throughout the depth of the pores. Checking the particular organization of the polymer backbone in the pores by polarized micro-Raman scattering failed because of a huge luminescence response of the sample. From the IRTF spectrum (Figure 5b), we can observe the presence of a shoulder at 1605 cm^{-1} characteristic of the stretching

vibration band of a double bond ($\nu_{C=C}$), which confirms the polymerization occurrence.

Polydiacetylene derivatives are well-known to be prepared by a topochemical polymerization.[46] This process requires an optimal packing of the monomer diacetylenic segments to allow the propagation in the solid state to make a conjugated backbone across the assembly, which explains a uniform polymerization in the porous layer.[47] Under those conditions of topochemical process, the pre-organization of the monomer in the pores (Scheme 1) should be maintained after the polymerization step and would thus lead to polymeric chains organized along the pore axis.

We have employed FTIR absorption spectroscopy to investigate the conformational order of the alkyl side chains as well as to probe the changes in molecular packing and bonding interaction of the lateral head groups after the polymerization process. The asymmetric $\nu_{as}(CH_2)$ and symmetric $\nu_s(CH_2)$ stretching vibrations remained unchanged in the polymer at 2917 and 2847 cm^{-1}, respectively (Figure 5b). This observation seems to indicate that a good degree

(42) Eckhardt, H.; Boudreaux, D. S.; Chance, R. R. *J. Chem. Phys.* **1986**, *85*, 4116.
(43) Mino, N.; Tamura, H.; Ogawa, K. *Langmuir* **1991**, *7*, 2336.
(44) Deckert, A. A.; Horne, J. C.; Valentine, B.; Kiernan, L.; Fallon, L. *Langmuir* **1995**, *11*, 643.
(45) Angkaew, S.; Wang, H.-Y.; Lando, J. B. *Chem. Mater.* **1994**, *6*, 1444.

(46) Tieke, B.; Lieser, G.; Wegner, G. *J. Polym. Sci.* **1979**, *17*, 1631.
(47) Bloor, D.; Chance, R. R. *Polydiacetylenes. Advances in Polymer Science*; Martinus Nijhoff: Boston, MA, 1985; Vol. 63.

of order of alkyl side chains is maintained after the polymerization process.

The FTIR spectra (Figure 5b) with a broad band around 3000 cm^{-1} corresponding to the headgroup region (−COOH) indicates that hydrogen bonding is also maintained in the polymer. The strong band found at 1697 cm^{-1} is assigned to carbonyl vibration ($\nu_{C=O}$). The location of this peak indicates strong head group hydrogen bonding as compared with the band of free carboxylic acid group at 1730 cm^{-1}.[48] Additionally, the presence of the O−H bending mode at 927 cm^{-1} characterizes the acid dimer form in the polymer. The presence of hydrogen bonding has been suggested to control the packing.[49] The polymerization process can provide some perturbations in supramolecular assemblies, leading to a decrease in alkyl side-chain arrangement in the polymer. However, hydrogen bonding may lock the head groups such that the alkyl side-chain organization is maintained or only partially perturbed during the topochemical polymerization process. The gauche−trans conformational change of the alkyl side chains imposes a strain on the polymer backbone, which can cause a reduction in the effective conjugated length of the ene−yne backbone and in turn the electronic properties of the polymer.[50] The Raman data that indicate a high conjugation length are consistent with a good packing of the pendent side chains.

Conclusion

Novel porous silicon nanocomposites have been synthesized using a dicarboxylic-acid-terminated diacetylenic monomer. The chemical nature of the porous silicon surface was found to have a strong impact on the pore filling. The self-assemblies embedded in the porous layer can polymerize in situ with UV irradiation to generate a blue-phase polymer.

Polarized Raman scattering provides information about the preferential orientation of the monomeric diacetylenic segment along the pore axis. IRTF data do not indicate any evidence of alkyl side chain disordering and suggest a well-organized polymer formation.

Hydrogen bonding and self-assembly of diacetylenic segments and the spatial confinement provided by the porous silicon matrix seem to be a good means to control the polymer chain organization and thus the nanocomposite properties. We are also currently extending the research to other self-assembled structures.

(48) Pimentel, G. C.; McClellan, A. L. *The Hydrogen Bond*; Reinhold Publishing Corporation: New York, 1960.
(49) Cheng, Q.; Yamamoto, M.; Stevens, R. C. *Langmuir* **2000**, *16*, 5333.
(50) Tomioka, Y.; Tanaka, N.; Imazeki, S. *J. Chem. Phys.* **1989**, *91*, 5694.